ANTIOXIDANTS & REDOX SIGNALING
Volume 32, Number 17, 2020

DOI: 10.1089/ars.2019.7879

FORUM ORIGINAL RESEARCH COMMUNICATION

Heme Oxygenase-1 Is a Pivotal Modulator of Bone Turnover and Remodeling: Molecular Implications for Prostate Cancer Bone Metastasis

Nicolás Anselmino,[1,2] Michael Starbuck,[3] Estefania Labanca,[3] Javier Cotignola,[1,2] Nora Navone,[3] Geraldine Gueron,[1,2] Ana C. Zenclussen,[4] and Elba Vazquez[1,2]

Abstract

Aims: Bone is the most frequent site of prostate cancer (PCa) metastasis. Tumor cells interact with the bone microenvironment interrupting tissue balance. Heme oxygenase-1 (HO-1; encoded by *Hmox1*) appears as a potential target in PCa maintaining the cellular homeostasis. Our hypothesis is that HO-1 is implicated in bone physiology and modulates the communication with PCa cells. Here we aimed at (i) assessing the physiological impact of *Hmox1* gene knockout (KO) on bone metabolism *in vivo* and (ii) determining the alterations of the transcriptional landscape associated with tumorigenesis and bone remodeling in cells growing in coculture (PCa cells with primary mouse osteoblasts [PMOs] from BALB/c $Hmox1^{+/+}$, $Hmox1^{+/-}$, and $Hmox1^{-/-}$ mice).

Results: Histomorphometric analysis of $Hmox1^{-/-}$ mice bones exhibited significantly decreased bone density with reduced remodeling parameters. A positive correlation between *Hmox1* expression and *Runx2*, *Col1a1*, *Csf1*, and *Opg genes* was observed in PMOs. Flow cytometry studies revealed two populations of PMOs with different reactive oxygen species (ROS) levels. The high ROS population was increased in PMOs $Hmox1^{+/-}$ compared with $Hmox1^{+/+}$, but was significantly reduced in PMOs $Hmox1^{-/-}$, suggesting restrained ROS tolerance in KO cells. Gene expression was altered in PMOs upon coculture with PCa cells, showing a pro-osteoclastic profile. Moreover, HO-1 induction in PCa cells growing in coculture with PMOs resulted in a significant modulation of key bone markers such as *PTHrP* and *OPG*.

Innovation and Conclusion: We here demonstrate the direct implications of HO-1 expression in bone remodeling and how it participates in the alterations in the communication between bone and prostate tumor cells. *Antioxid. Redox Signal*. 32, 1243–1258.

Keywords: *HMOX1*, bone remodeling, prostate cancer, osteoblasts, osteoclasts

[1]Laboratorio de inflamación y Cáncer, Departamento de Química Biológica, Facultad de Ciencias Exactas y Naturales, Universidad de Buenos Aires, Buenos Aires, Argentina.
[2]Instituto de Química Biológica de la Facultad de Ciencias Exactas y Naturales (IQUIBICEN), CONICET—Universidad de Buenos Aires, Buenos Aires, Argentina.
[3]Department of Genitourinary Medical Oncology, The University of Texas MD Anderson Cancer Center, Houston, Texas, USA.
[4]Experimental Obstetrics and Gynecology, Medical Faculty, Otto-von-Guericke University Magdeburg, Magdeburg, Germany.
Part of the abstract of this work was published in Medicina 78(Suppl III): 51, 2018.

Innovation

Advanced prostate cancer exhibits bone dissemination as the preferable site for metastasis accompanied by an average survival of $\sim$40 months. Bone metastases are incurable and only palliative treatments are available. Our results showcase for the first time the direct effect of the heme oxygenase-1 gene (*Hmox1* gene) on bone turnover and remodeling and demonstrate that its modulation on both prostate tumor cells and bone cells changes their communication altering the tumoral bone niche. A better understanding of how these processes influence the early onset of bone metastasis can shed light into more tailored therapies.

Introduction

Prostate cancer (PCa) is the second-most frequently diagnosed cancer and the fifth leading cause of cancer-related deaths in men worldwide (5a). PCa progression is dominated by a constant tumor adaptation (32, 40). The acquisition of resistance to androgen deprivation therapy coincides with PCa bone metastases in most cases, indicating the presence of a bone/epithelial interaction that drives organ-specific progression. Bidirectional interaction between bone cells and PCa cells suggests that not only growth factors derived from the tumor can affect bone cells but also that cells from the bone microenvironment stimulate metastatic tumor growth (32, 37, 62).

Bone is a mineralized connective tissue that has four main cell types: osteoblasts, bone ''lining'' cells, osteocytes, and osteoclasts (14). This tissue has important functions such as locomotion, support and protection of soft tissues, calcium and phosphate reservoir, and bone marrow shelter (12, 52). Bone is a highly dynamic organ that is continuously degraded by osteoclasts and regenerated by osteoblasts (5, 9, 33, 56).

Osteoblasts are responsible for bone formation, synthesizing and secreting proteins to form the osteoid, which will then be mineralized and converted to mature bone (11). These cells derive from mesenchymal stem cells (MSCs), which can also be differentiated to other cell types, including adipocytes and chondrocytes (51). The commitment of MSCs toward a lineage of bone progenitor cells requires the expression of specific genes, followed by temporarily programmed steps that include the synthesis of bone morphogenetic proteins (BMPs) and members of the Wnt pathway (18). The expression of Runt-related transcription factor 2 (Runx2), Dlx5, and Osx is crucial for osteoblast differentiation (7, 64).

Osteoclasts are differentiated multinucleated cells that originate from mononuclear cells of hematopoietic stem cell lineage, under the influence of several factors (25). These factors include the macrophage colony stimulating factor (M-CSF or CSF-1), secreted by bone progenitor mesenchymal cells and osteoblasts, and RANKL (receptor activator for nuclear factor κ B ligand), secreted by osteoblasts, osteocytes, and stromal cells (42). The RANKL/RANK (receptor activator for nuclear factor κ B)/OPG (osteoprotegerin) axis is the main mediator of osteoclastogenesis (49).

The bone remodeling process is a highly complex cycle that is carried out by the concerted action of the cell types described above (52). Systemic factors for bone homeostasis maintenance include parathyroid hormone (PTH), calcitonin, 1,25-dihydroxy vitamin D3 (calcitriol), glucocorticoids, androgens, and estrogens (6, 36, 59, 70). PTH-related protein (PTHrP), which also binds to the PTH receptor, has been reported to influence bone remodeling (6).

PCa cell bone affinity may owe to the expression of genes that predispose cells to lodge in the bone marrow, although it is also possible that these cells acquire osteomimetic properties after being located within the bone compartment. Once in the bone, disseminated tumor cells or their progeny may have osteoblastic, osteoclastic, or both effects (13, 54). Metastatic tumor cells are not the only ones responsible for inducing bone destruction/formation. This process mainly involves osteoblasts and osteoclasts. PTHrP, interleukin (IL)-1, IL-6, and prostaglandin E2 (PGE2) can regulate the osteoblast production of RANKL/OPG and modulate osteoclast activation (44).

The concept that there are basically two types of bone metastases—osteoblastic or osteoclastic—might be too simplistic. The processes of resorption and bone formation are usually linked or coupled. There is plenty of evidence that both processes are activated in the majority of bone metastases (44).

Reactive oxygen species (ROS) can cause severe tissue damage due to the accumulation of changes in vital macromolecules. Currently, the mechanisms by which cells sense pro-oxidant states and activate signaling pathways to counteract changes are not completely known. However, the expression of heme oxygenase (HO) family enzymes (heme catabolizers) is a well-preserved strategy throughout evolution to counteract ROS (39).

HO-1 is a 32 kDa protein inducible through a variety of stimuli, including ROS and inflammatory cytokines (46). It is well known that inflammation favors PCa and its progression (41). Proinflammatory factors secreted by PCa and bone cells and the subsequent release of bone matrix factors mediate the paracrine/autocrine interaction between PCa cells, osteoblasts, and osteoclasts, ultimately determining the bone phenotype and PCa progression (15, 22). Oxidative stress is a natural consequence of the inflammatory process and acts as a modulator for the mineralized tissue function (63).

We previously demonstrated that HO-1 participates in PCa bone metastasis, restoring osteoblast proliferation (16), which was shown to be significantly inhibited by coculturing PC3 cells with primary mouse osteoblasts (PMOs) (67). We also found that HO-1 is capable of modulating signaling pathways relevant to bone metastasis, such as FoxO/β-catenin, and promotes bone remodeling when tumor cells are transplanted into the femur of SCID mice (16). More recently, we reported that HO-1 modulates cellular adhesions in PCa, increasing E-cadherin and β-catenin levels and its subsequent relocation to the plasma membrane, favoring a more epithelial phenotype (21).

We also reported that HO-1 induction alters the expression of different cytoskeletal genes and is associated with key factors that induce the remodeling of actin filaments in the filopodia, increasing adhesion and decreasing PCa cell invasiveness (48). However, the effect of HO-1 deficiency in the bone physiology and in the communication between PCa cells and cells of the bone stroma is yet to be fully explored.

Here, we thoroughly describe the direct effect of heme oxygenase-1 gene (*Hmox1*) total, partial, or absent expression in impairing bone turnover and remodeling. We further

established coculture system models of human PCa cells with PMOs from *Hmox1* transgenic mice, and delineated a set of osteoblastic and osteolytic genes (*PTHrP*, *OPG*, and *RANKL*) and analyzed how HO-1 expression levels affected this signature.

Results

Morphological, genetic, and physiological characterization of bone from knockout Hmox1 *mice*

We have previously used a coculture system of PC3 cells with PMOs to show that the decrease in PMO proliferation induced by tumor cells was restored when these cells were treated with hemin, a specific pharmacological inducer of HO-1. Hemin treatment increased the expression of DKK1 (inhibitor of Wnt/β-catenin pathway in bone remodeling) in cocultured PC3 cells, redirecting β-catenin toward the FoxO pathway in osteoblasts and activating the transcription of factors involved in counteracting oxidative stress. In addition, the intrabone inoculation of PCa cells overexpressing HO-1 (PC3HO-1) produced a robust bone remodeling (16). These findings suggested that HO-1 plays a key role in the control of inflammation, oxidative stress, and angiogenesis, which in turn altered the tumor microenvironment impacting on PCa bone progression.

In this work, we evaluated by histomorphometric analysis of femurs from male BALB/c $Hmox1^{+/+}$ (wild-type [WT]); $Hmox1^{+/-}$ (heterozygous [Het]); $Hmox1^{-/-}$ (knockout [KO]) mice, the involvement of HO-1 on bone remodeling. We also investigated the role of HO-1 deficiency in the communication through released soluble factors between osteoblasts and prostatic cancer cells, using a coculture system of PMOs isolated from the calvaria of the *Hmox1* transgenic animals and PC3 cells.

Histomorphometric analysis of femurs of the different groups was carried out to characterize the animal model and evaluate whether the different genetic backgrounds resulted in alterations in the physiology and, therefore, in the morphology of the bone tissue. Our results showed a significant decrease in bone volume, bone density, and trabecular bone density, with an increase in the average distance between trabeculae, in the $Hmox1^{-/-}$ *versus* $Hmox1^{+/+}$ animals (Figs. 1 and 2A). In agreement with these results, a reduction was also seen in all the static parameters of bone formation, with a total loss of the osteoid surface (OS; used as a bone neoformation parameter), consistent with a reduction in the number of osteoblasts (Figs. 1A and 2B). Accordingly, a decrease in osteoclast number was observed, and the consequent reduction of the static resorption parameters (Figs. 1B and 2C).

Considering the differences observed at the morphological level, we next sought to evaluate if these alterations could be explained by changes in the expression of genes related to bone metabolism. For this purpose, PMOs were isolated from the calvaria of the $Hmox1^{+/+}$, $Hmox1^{+/-}$, and $Hmox1^{-/-}$ animals, and the expression of genes involved in bone physiology was analyzed by real-time quantitative polymerase chain reaction (RT-qPCR). We found a direct correlation between expression levels of *Hmox1* and genes such as *Runx2*—osteoblast early differentiation associated gene—*Col1a1*—involved in the deposition of the collagen matrix—and *Csf-1*, *Opg*—secretion proteins that modulate osteoclast differentiation/activation (Fig. 3A). Other critical molecules involved in the activation and function of osteoclasts, such as *Opn*—mediates osteoclast adhesion for bone resorption—*Il-6*—osteoclast differentiation/activation modulator—and *Rankl*—osteoclast differentiation factor, showed a behavioral pattern independent of *Hmox1* levels (Fig. 3A).

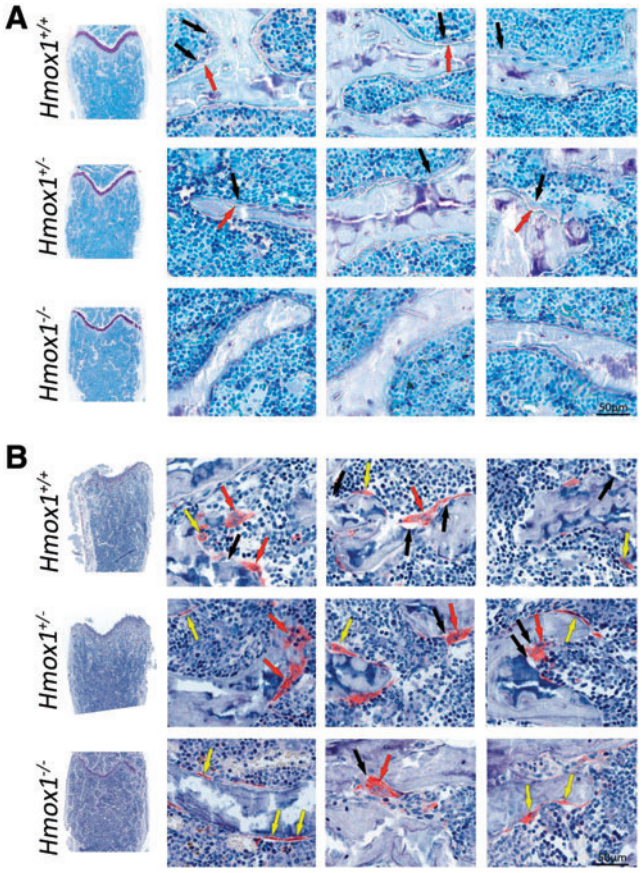

FIG. 1. Histological section of femurs of BALB/c $Hmox1^{+/+}$, $Hmox1^{+/-}$, and $Hmox1^{-/-}$ mice. (A) Staining with toluidine blue for the analysis of osteoblasts (*black arrows*) and osteoid (*red arrows*); or **(B)** staining for TRAP. *Red arrows* indicate mature osteoclasts, *yellow arrows* indicate monocytes, and *black arrows* show eroded areas. The images at the *left column* are montages of images taken with 20× objective. *Hmox1*, heme oxygenase-1 gene; TRAP, acid phosphatase tartrate resistant. Color images are available online.

It was previously reported that HO-1 confers cytoprotection against inflammation and oxidative stress in several animal models (20). Oxidative stress is a natural consequence of the inflammatory process and acts as a modulator of the function of mineralized tissues (63). This impacts bone formation by inhibiting osteoblast differentiation and by promoting apoptosis (2). These effects are mediated, in part, by ROS generated in the context of oxidative stress. Taking this into account, we next evaluated ROS levels in PMOs obtained from $Hmox1^{+/+}$, $Hmox1^{+/-}$, and $Hmox1^{-/-}$ mice by flow cytometry (Fig. 3B). A lower percentage of DCF+ cells in the $Hmox1^{-/-}$ PMOs were observed when compared with those from the $Hmox1^{+/+}$ or $Hmox1^{+/-}$ animals (Fig. 3B.I). When analyzing the frequency distribution for the DCF

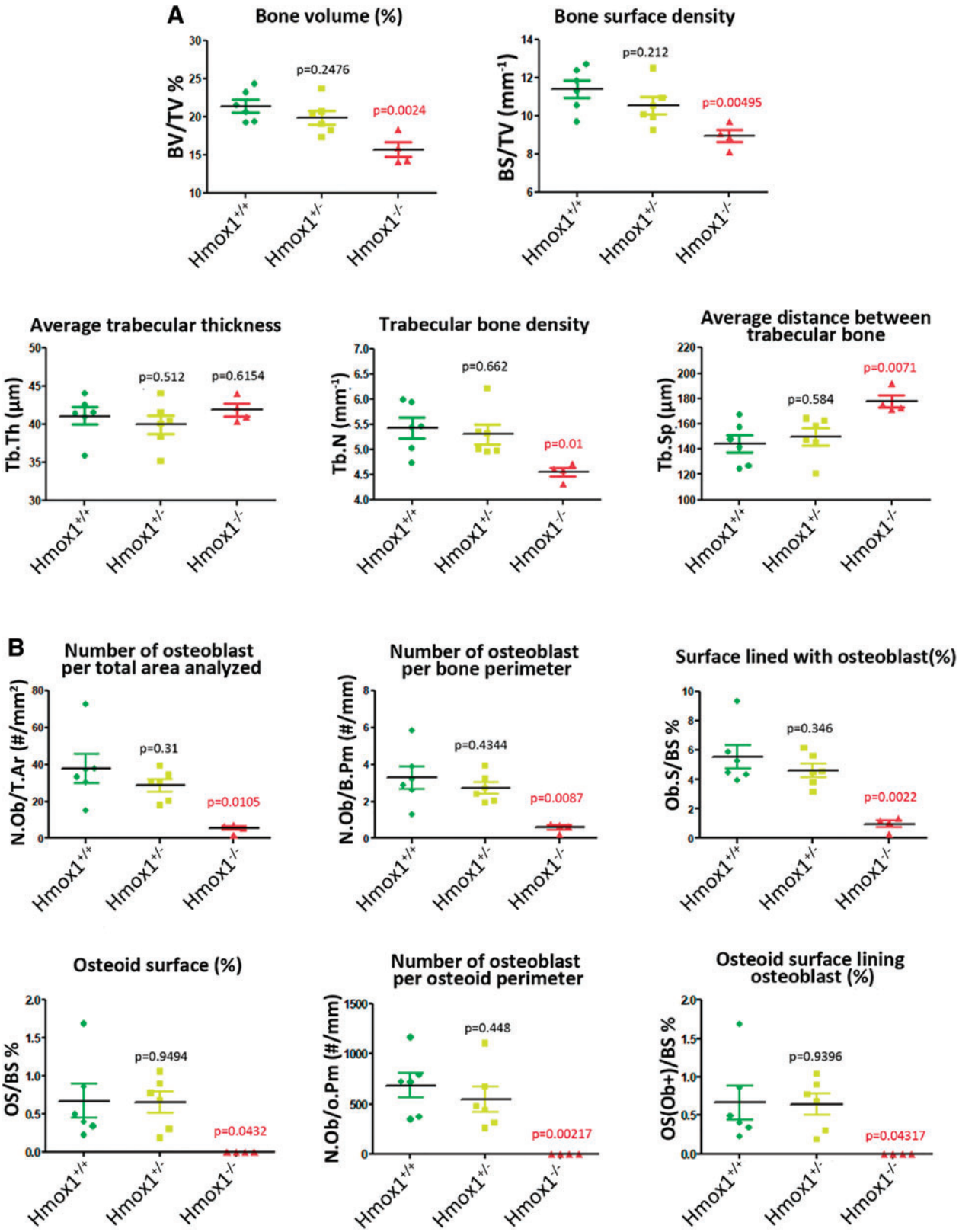

FIG. 2. Histomorphometry analysis of femurs of BALB/c *Hmox1*$^{+/+}$ (WT), *Hmox*$^{+/-}$ (Het); *Hmox1*$^{-/-}$ (KO) mice. Dot-plot graphs depicting **(A)** different bone structural parameters, **(B)** static formation parameters and **(C)** static resorption parameters. In each case, the statistical significance (*p* value) is expressed with respect to the values obtained for the WT animals. *p* Value in *red* indicates significant differences. BS/TV, bone surface/tissue volume; BV/TV, bone volume/tissue volume; ES/BS, eroded surface/bone surface; N.Ob/B.Pm, osteoblasts/bone perimeter; N.Ob/O.Pm, osteoblasts/osteoid perimeter; N.Ob/T.A, osteoblasts/total area; N.Oc/B.Pm, osteoclasts/bone perimeter; N.Oc/B.Pm, osteoclasts/bone perimeter; N.Oc/T.A, osteoclasts/total area; Ob.S/BS, osteoblast surface/bone surface; OS/BS, osteoid surface/bone surface; Os(Ob+)/BS, osteoid surface lined with osteoblast/bone surface; Tb.N, trabecular number; Tb.Sp, trabecular separation; Tb.Th, trabecular thickness; WT, wild type. Color images are available online.

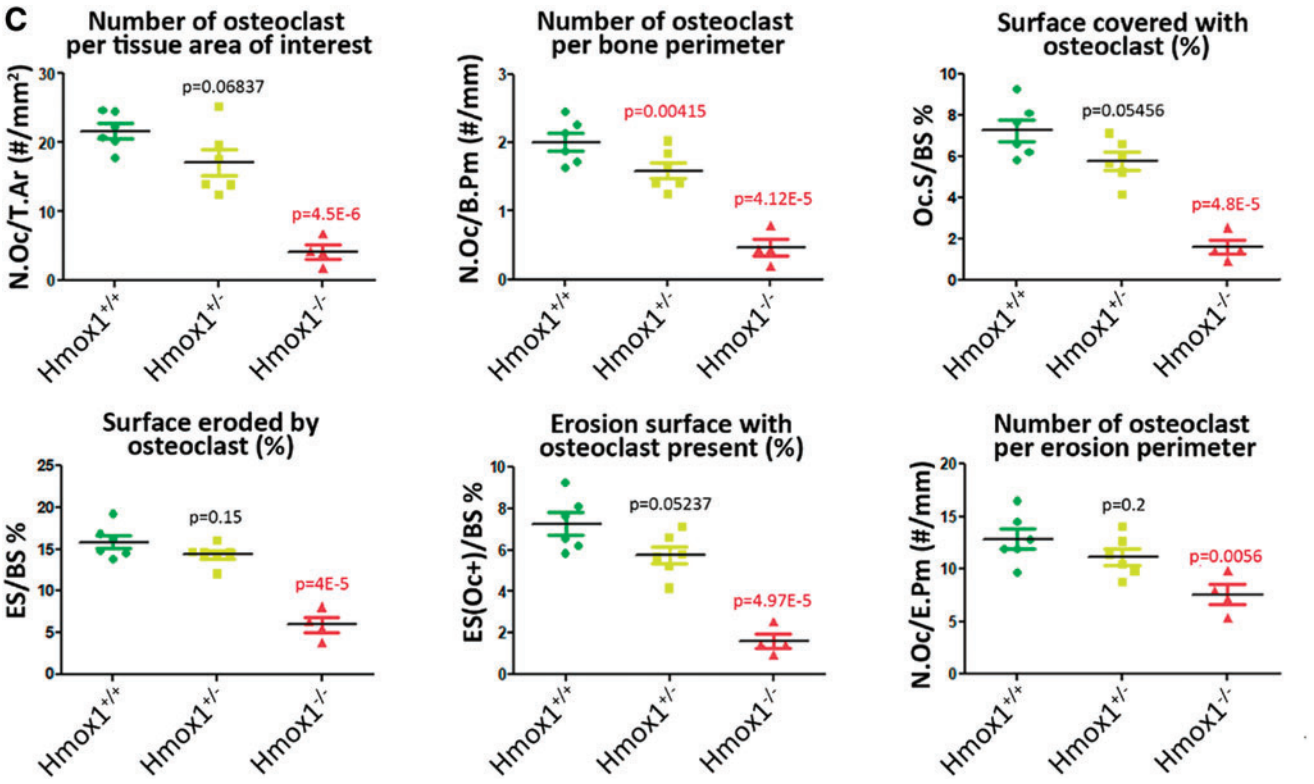

FIG. 2. (*continued*).

signal intensity (Fig. 3B.II), we identified two cell populations: ''High'' and ''Low.'' In addition, the ''Low'' population of *Hmox1*$^{+/-}$ and *Hmox1*$^{-/-}$ cells had a slightly lower fluorescence intensity compared with *Hmox1*$^{+/+}$ PMOs. On the contrary, the ''High'' populations had the same intensity, but the frequency was higher in *Hmox1*$^{+/-}$ PMOs when compared with the *Hmox1*$^{+/+}$ PMOs. The frequency of cells in the ''High'' population for the *Hmox1*$^{-/-}$ PMOs was barely present (Fig. 3B.III). Overall, these results might suggest that in the PMOs from the *Hmox1* heterozygous animals, the increase in the ''High'' population might be due to the fact that these cells had fewer copies of *Hmox1* (compared with WT animals), and therefore, a decreased ability to maintain redox homeostasis. In addition, in the case of Hmox1$^{-/-}$ PMOs, a striking decrease in the ''High'' population was observed, indicating that HO-1 loss might establish a maximum limit in ROS level tolerance for these cells. However, we cannot discard the possibility that the imbalance in the antioxidant state, produced as a consequence of *Hmox1* loss, could trigger the activation of other antioxidant pathways.

Role of Hmox1 *expression in osteoblasts upon interaction with PCa cells*

Given the morphological, physiological, and genetic differences observed in the bones of animals with the different *Hmox1* genetic backgrounds, we next analyzed the effect of the coculture of PC3 cells (pretreated or not with hemin, specific HO-1 chemical inducer) with PMOs isolated from *Hmox1*$^{+/+}$, *Hmox1*$^{+/-}$, and *Hmox1*$^{-/-}$ animals to understand the relevance of HO-1 in bone metastases.

First, we compared ROS levels in PMOs from the three groups of animals between the different coculture conditions (Fig. 4A). Only the *Hmox1*$^{+/-}$ PMOs showed an increase in the percentage of DCF+ cells when cocultured with PCa cells, whether they were pretreated or not with hemin (Fig. 4B). Considering the results from Figures 3B and 4, the stressor effect generated by the presence of PCa cells was evident only in *Hmox1*$^{+/-}$ PMOs due to the diminished regulatory capacity. It is possible given that *Hmox1* levels are lower in *Hmox1*$^{+/-}$ compared with WT animals, this decrease in *Hmox1* expression may have more significant consequences, evidenced by increased ROS levels in these cells.

Taking into consideration that a decrease in *Hmox1* levels is also seen in WT animals, this reduction in *Hmox1* net levels may not be as lower as in *Hmox1*$^{+/-}$ animals, and hence may be sufficient enough to counteract oxidative stress. The next step was to evaluate *Hmox1* gene expression in the coculture system. Messenger RNA (mRNA) levels of *Hmox1* in both the *Hmox1*$^{+/+}$ and *Hmox1*$^{+/-}$ PMOs were negatively modulated upon coculture with PC3 cells (pretreated or not with hemin) (Fig. 4C.II, III). Given that *Hmox1* expression levels in PMO KO were extremely low (Fig. 4C.I), RT-qPCR quantification for this gene in PMO KO cocultured with PC3 cells was not sensitive enough for an accurate *Hmox1* determination.

When analyzing the coculture effect on the expression of bone remodeling genes (Fig. 5A) in the *Hmox1*$^{+/+}$ PMOs, we found that the presence of tumor cells had a negative impact on *Opg* and *Csf-1* expression, and this effect was maintained when PCa cells were pretreated with hemin (Fig. 5B–D). Furthermore, *Rankl* expression was positively regulated by the coculture (Fig. 5). This increase in addition to the

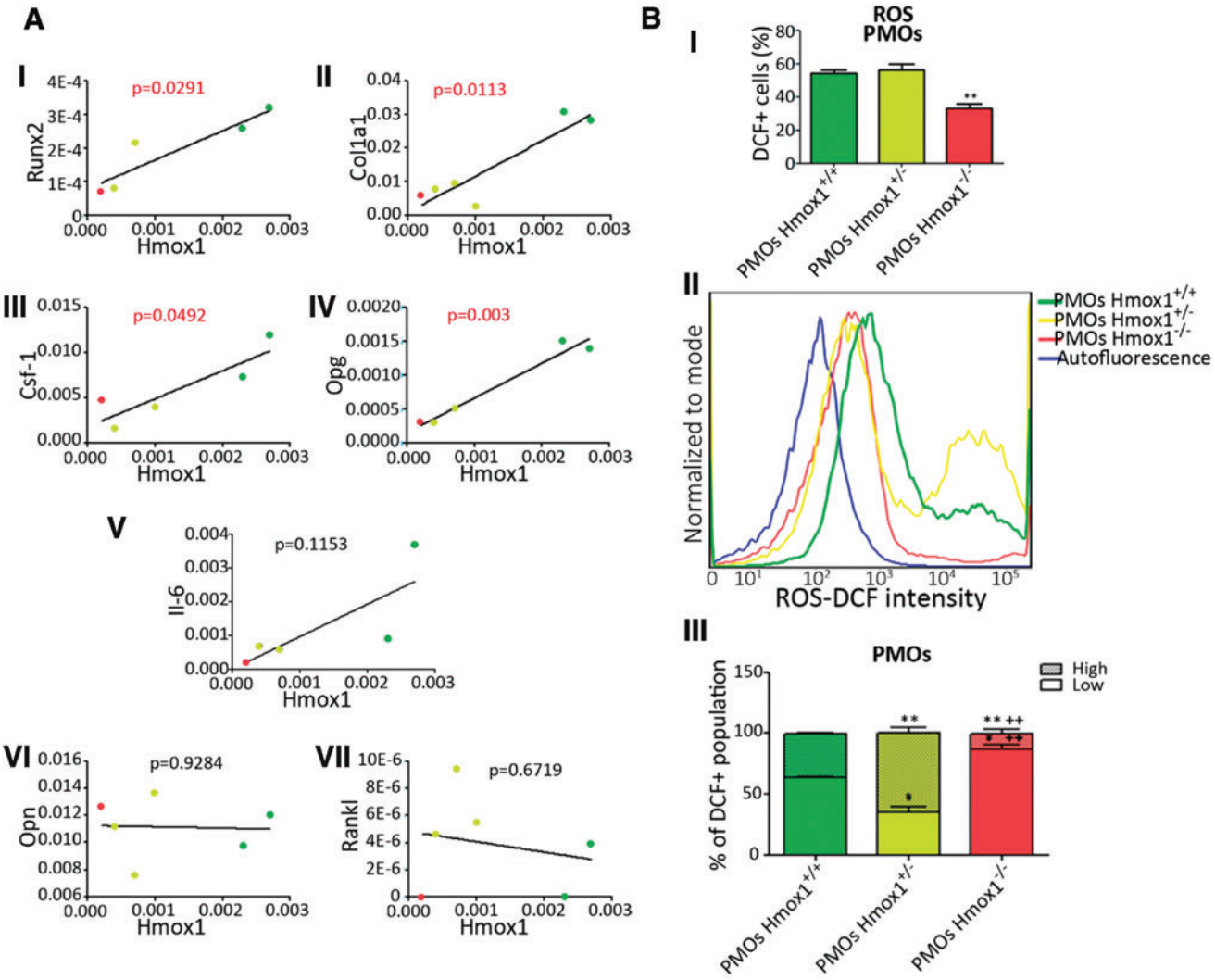

FIG. 3. Expression of bone remodeling genes and oxidative stress levels in primary mouse osteoblasts isolated from *Hmox1*$^{+/+}$, *Hmox1*$^{+/-}$; *Hmox1*$^{-/-}$ mice calvariae. (A) Correlation in the expression of genes involved in bone remodeling with respect to *Hmox1*. Gene expression levels (relative to *36b4*) measured by RT-qPCR: **(I)** *Runx2*; **(II)** *Col1a1*; **(III)** *Csf-1*; **(IV)** *Opg*; **(V)** *Il-6*; **(VI)** *Opn* and **(VII)** *Rankl*, expressed as a function of the levels of *Hmox1* in PMOs isolated from BALB/c *Hmox1*$^{+/+}$, *Hmox1*$^{+/-}$, and *Hmox1*$^{-/-}$ mice. *Color* of the *dots* represents the specific genotype of the *Hmox1*$^{+/+}$ (*green dots*), *Hmox1*$^{+/-}$ (*yellow dots*), and *Hmox1*$^{-/-}$ (*red dots*). The data were subjected to a linear regression. In each case, the statistical significance (*p* value) is expressed for the linear regression obtained. *p* Value in *red* indicates significant differences. **(B)** ROS levels in PMOs measured by flow cytometry in the FITC channel, using DCFDA as a probe. **(I)** shows the percentage of FITC+ cells for PMOs *Hmox1*$^{+/+}$, *Hmox1*$^{+/-}$, *Hmox1*$^{-/-}$; **(II)** shows a representative histogram for FITC intensity for PMOs *Hmox1*$^{+/+}$ (*green*), *Hmox1*$^{+/-}$ (*yellow*), *Hmox1*$^{-/-}$ (*red*), and autofluorescence (*blue*); **(III)** shows the percentage distribution of FITC+ cells in each intensity population (High or Low). Results are expressed as mean ± SD. *Hmox1*$^{+/+}$: $^{*}p<0.05$; $^{**}p<0.01$. Statistical difference with respect to the PMOs *Hmox1*$^{+/-}$; $^{++}p<0.05$. Col1a1, collagen type I alpha 1 chain; CSF-1, colony stimulating factor 1; DCFDA, 5-(and-6)-carboxy-2′,7′-dichlorofluorescein diacetate; FITC, fluorescein isothiocyanate; PMOs, primary mouse osteoblasts; ROS, reactive oxygen species; RT-qPCR, real-time quantitative polymerase chain reaction; SD, standard deviation. Color images are available online.

decrease in *Opg* would cause an imbalance in the Rankl/Opg ratio that might favor the osteoclast activation in the bone microenvironment (Fig. 5A). Although hemin pretreatment of tumor cells had no further effect on *Opg* expression in *Hmox1*$^{+/+}$ PMOs after coculture, it was able to prevent the increase in *Rankl* expression. In line with this, the coculture with PCa cells pretreated with hemin induced an increase in the expression of *Runx2* in *Hmox1*$^{+/+}$ PMOs (Fig. 5B), leading toward a less pro-osteoclastic profile. Other genes such as *Il-6* suffered a small decrease, which was only significant compared with the coculture with PC3 cells pretreated with hemin (Fig. 5B). *Col1a1* and *Opn* were not affected in any of the assayed conditions (Fig. 5B).

Regarding *Opg*, *Runx2*, *Csf-1*, and *Opn* expression in *Hmox1*$^{+/-}$ PMOs (Fig. 5C), we observed the same effect described for *Hmox1*$^{+/+}$ PMOs. These results suggest that the response is not affected by *Hmox1* basal levels in bone cells. Moreover, even in *Hmox1*$^{-/-}$ PMOs, the coculture effects on

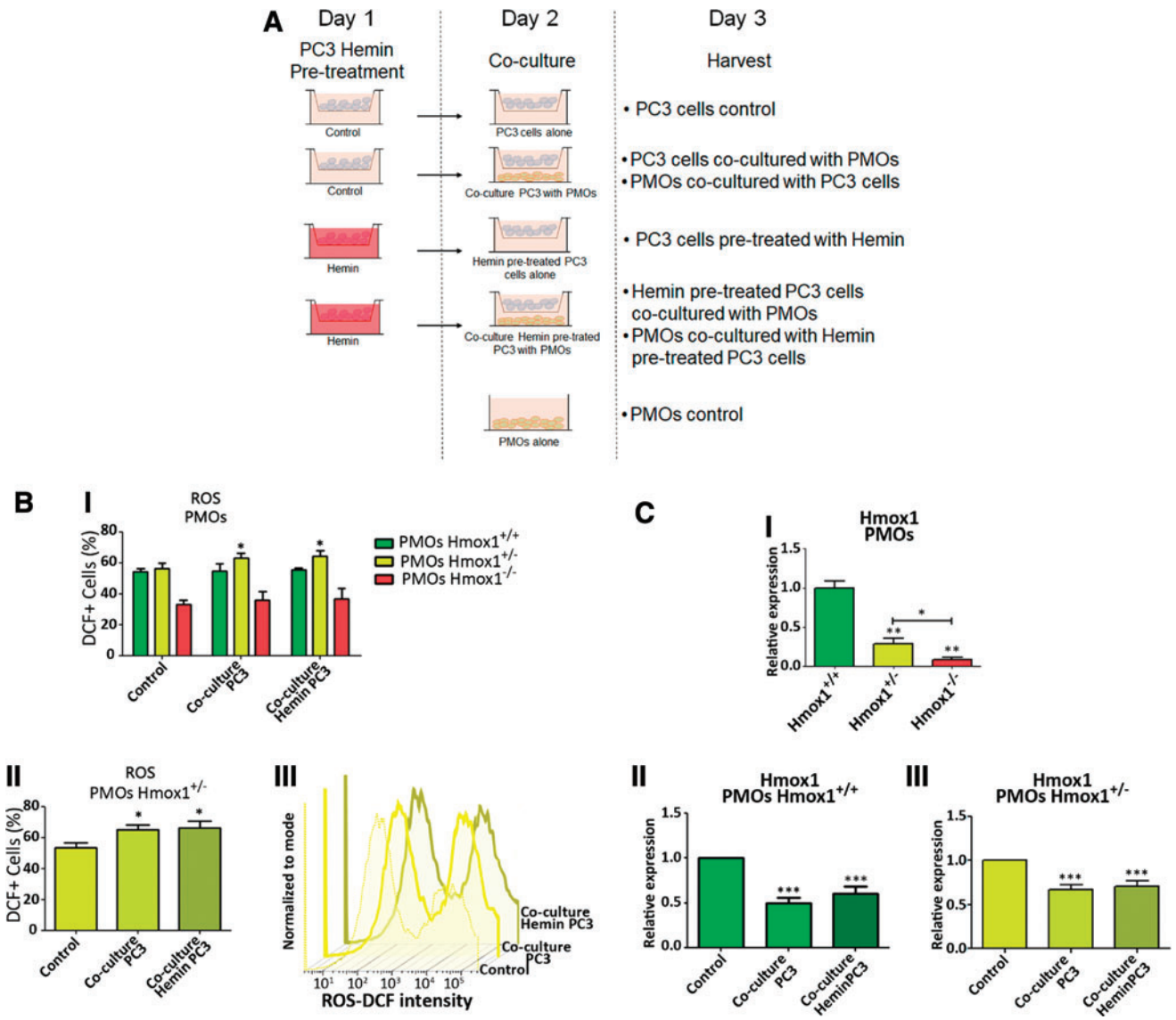

FIG. 4. Co-culture of primary mouse osteoblasts isolated from *Hmox1*$^{+/+}$, *Hmox1*$^{+/-}$, *Hmox1*$^{-/-}$ mice calvaria and PC3 cells. (A) Coculture system representation. **(B)** *Upper panel* **(I)** depicts levels of ROS measured in PMOs (*Hmox1*$^{+/+}$, *Hmox1*$^{+/-}$, *Hmox1*$^{-/-}$) under the different coculture conditions by flow cytometry, in the FITC channel using a DCFDA probe. *Lower left panel* **(II)** shows FITC+ cells in *Hmox1*$^{+/-}$ PMOs cultured under the experimental conditions detailed in the figure. *Lower right panel* **(III)** shows representative histograms for the intensity of FITC in PMOs *Hmox1*$^{+/-}$ in the coculture experimental conditions. $*p<0.05$. **(C)** *Upper panel* **(I)** shows the expression levels of *Hmox1* assessed by RT-qPCR in PMOs. *Lower panels* show the coculture effect with PC3 cells or PC3 cells pretreated with hemin (50 μM; 24 h), on the expression of *Hmox1* in PMOs **(II)** *Hmox1*$^{+/+}$ or **(III)** *Hmox1*$^{+/-}$. The values were relativized using *36B4* as a reference gene and normalized with respect to the control condition. Results are expressed as mean ± SD. $*p<0.05$; $**p<0.01$; $***p<0.001$. Color images are available online.

Opg, *Runx2*, and *Opn* expression are preserved, whereas the expression of *Csf-1* is only affected by the presence of tumor cells pretreated with hemin (Fig. 5D). The loss of *Hmox1* avoided the effect of the coculture on *Il-6* expression, evidenced by the lack of changes in *Hmox1*$^{+/-}$ and *Hmox1*$^{-/-}$ PMOs, under the tested conditions (Fig. 5C, D). Conversely, an increase in *Col1a1* expression was evident in *Hmox1*$^{+/-}$ PMOs when cocultured in the presence of hemin pretreated PC3 cells (Fig. 5C). This change in *Col1a1* expression could be evidenced in *Hmox1*$^{+/-}$ PMOs due to the lower basal levels of

FIG. 5. Expression of bone remodeling genes under co-culture of primary mouse osteoblasts isolated from *Hmox1*$^{+/+}$, *Hmox1*$^{+/-}$, *Hmox1*$^{-/-}$ mice calvaria and PC3 cells. (A) Schematic representation of soluble factors implicated in the communication between PCa and bone cells. Expression levels of **(I)** *Opg*, **(II)** *Rankl*, **(III)** *Runx2*, **(IV)** *Col1a1*, **(V)** *Csf-1*, **(VI)** *Il-6*, and **(VII)** *Opn* assessed by RT-qPCR in **(B)** *Hmox1*$^{+/+}$ PMOs, **(C)** *Hmox1*$^{+/-}$ PMOs, or **(D)** *Hmox1*$^{-/-}$ PMOs grown alone or in coculture with PC3 cells or PC3 cells pretreated with hemin (50 μM; 24 h). The values were relativized using *36B4* as a reference gene and normalized with respect to the control condition. Results are expressed as mean ± SD. $*p<0.05$; $**p<0.01$; $***p<0.001$. PCa, prostate cancer. Color images are available online.

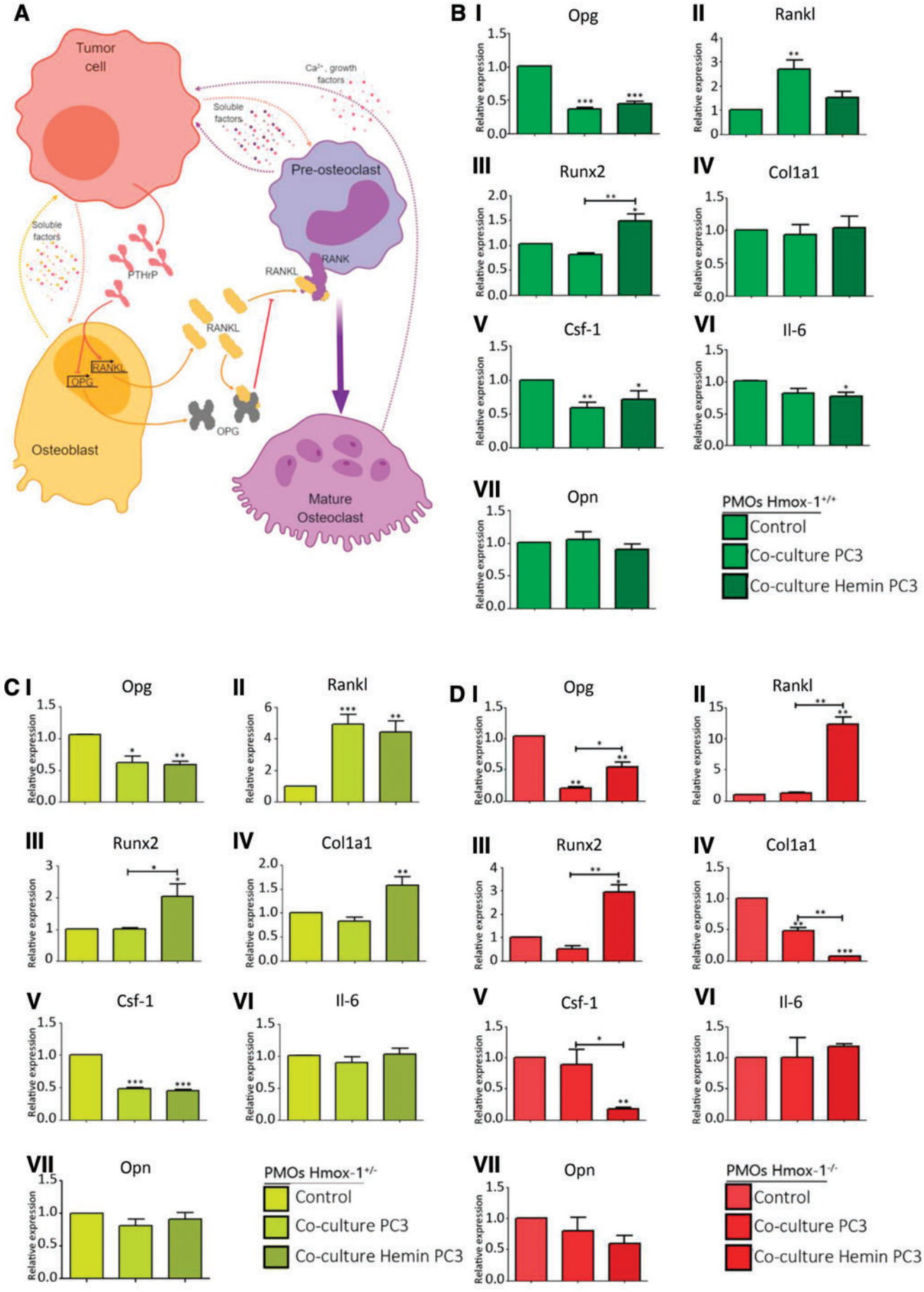
A
Tumor cell
Ca2+, growth factors
Soluble factors
Pre-osteoclast
Soluble factors
PTHrP
RANK
RANKL
RANKL
RANKL
OPG
OPG
Osteoblast
Mature Osteoclast
B I Opg
II Rankl
III Runx2
IV Col1a1
V Csf-1
VI Il-6
VII Opn
Relative expression
PMOs Hmox-1+/+
Control
Co-culture PC3
Co-culture Hemin PC3
C I Opg
II Rankl
III Runx2
IV Col1a1
V Csf-1
VI Il-6
VII Opn
PMOs Hmox-1+/-
Control
Co-culture PC3
Co-culture Hemin PC3
D I Opg
II Rankl
III Runx2
IV Col1a1
V Csf-1
VI Il-6
VII Opn
PMOs Hmox-1-/-
Control
Co-culture PC3
Co-culture Hemin PC3

this gene with respect to *Hmox1*$^{+/+}$ PMOs. In the case of *Hmox1*$^{-/-}$ PMOs, both experimental conditions led to a decrease in the expression of *Col1a1* (Fig. 5D), showing a change in the coculture effect due to the lack of HO-1 in PMOs.

Although the increase in *Rankl* expression due to the coculture effect with PCa cells is still observed in *Hmox1*$^{+/-}$ PMOs (Fig. 5C), the coculture with hemin pretreated tumor cells was not able to prevent *Rankl* induction, as observed in *Hmox1*$^{+/+}$ PMOs. On the contrary, the coculture with PCa cells was not able to induce the expression of *Rankl* in osteoblasts lacking *Hmox1*, while the presence of hemin pretreated tumor cells caused a significant overexpression of *Rankl* in *Hmox1*$^{-/-}$ PMOs (Fig. 5D). These results imply that the coculture effect on *Rankl* expression is modulated by HO-1 not only in the tumor cell but also in the osteoblast.

In the same way, the effect of the coculture was assessed in PCa cells. First, *HMOX1* levels were measured, resulting in no significant alteration when the tumor cells were cocultured with the PMOs (Fig. 6A). When tumor cells were pretreated with hemin, the induction of *HMOX1* was maintained in comparison with the coculture with *Hmox1*$^{+/+}$ PMOs, while the coculture with both *Hmox1*$^{+/-}$ and *Hmox1*$^{-/-}$ PMOs partially reversed the effect of the hemin pretreatment on *HMOX1* levels in the PCa cells (Fig. 6A).

As previously mentioned, *PTHrP* can be produced by tumor cells with implications not only for the tumor cell but for bone physiology as well (44). Under our experimental conditions, *PTHrP* expression was increased in PC3 cells cocultured with PMOs, independent of the genotype (Fig. 6B). Hemin pretreatment was able to prevent the induction of *PTHrP* in the coculture with *Hmox1*$^{+/+}$ PMOs. This preventive capacity of hemin pretreatment was not only lost when tumor cells were cocultured with *Hmox1*$^{+/-}$ PMOs but also enhanced the coculture effect when tumor cells were grown in the presence of *Hmox1*$^{-/-}$ PMOs (Fig. 6B).

The PC3 cells express *OPG* (27). As observed for *PTHrP*, *OPG* expression increased in tumor cells that had been cocultured with *Hmox1*$^{+/+}$ or *Hmox1*$^{+/-}$ PMOs, and this effect was prevented by hemin pretreatment (Fig. 6C). Besides, the coculture with *Hmox1*$^{-/-}$ PMOs negatively affected the expression of *OPG* in the tumor cells, independently of whether they had been pretreated with hemin (Fig. 6C).

In the case of DKK1, a critical factor in bone remodeling, acting as an inhibitor of the Wnt/β-catenin pathway (45), its expression was upregulated in tumor cells cocultured with *Hmox1*$^{+/+}$ or *Hmox1*$^{+/-}$ PMOs, but not when cocultured with *Hmox1*$^{-/-}$ PMOs (Fig. 6D).

In summary, hemin pretreatment modulated the response of tumor cells to the coculture with the PMOs, and this modulation was different depending on the PMO *Hmox1* genetic background. This clearly suggests that the HO-1 level in the PMOs is not only important for their physiology but is also relevant for their interaction with the tumor cells.

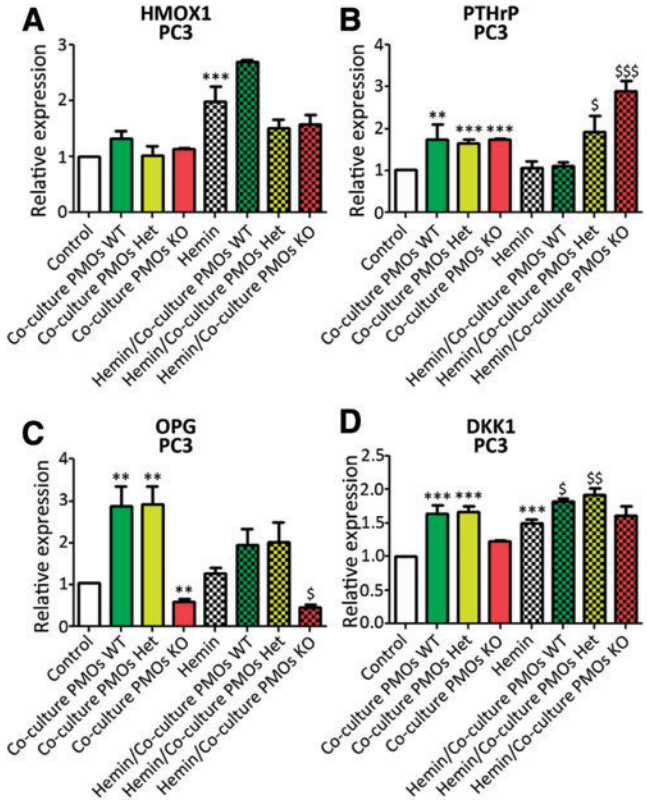

FIG. 6. Gene expression analyses in PC3 cells growing in co-cutlure with primary mouse osteoblasts isolated from *Hmox1*$^{+/+}$, *Hmox1*$^{+/-}$, *Hmox1*$^{-/-}$ mice calvaria. Expression levels of **(A)** *HMOX1*, **(B)** *PTHrP*, **(C)** *OPG*, and **(D)** *DKK1*, assessed by RT-qPCR in PC3 cells pretreated or not with hemin (50 μM; 24 h), grown alone or in coculture (24 h) with PMOs *Hmox1*$^{+/+}$; *Hmox1*$^{+/-}$; and *Hmox1*$^{-/-}$. The values were relativized using *PPIA* as a reference gene and normalized with respect to the control condition. Results are expressed as mean ± SD. Statistical significance with respect to control: $^{**}p < 0.01$; $^{***}p < 0.001$; or hemin: $^{\$}p < 0.05$; $^{\$\$}p < 0.01$; $^{\$\$\$}p < 0.001$. DKK1, inhibitor of Wnt/β-catenin pathway in bone remodeling. Color images are available online.

Discussion

Bone is a dynamic tissue that undergoes homeostatic remodeling mediated by the balanced activities of osteoblasts and osteoclasts (34). HO-1 plays a critical role in the physiology of this process (34, 55, 61). HO-1 was shown to maintain bone mass during physiological bone remodeling (34).

The histomorphometric analysis of mice femurs for the different genetic backgrounds (*Hmox1*$^{+/+}$, *Hmox1*$^{+/-}$, and *Hmox1*$^{-/-}$) presented in this work showed a decrease in bone volume concomitant with the loss of *Hmox1*. In line, a lower number of osteoblasts were observed, with the consequent reduction of osteogenic parameters. These results are consistent with the functions previously described for HO-1 (4, 60, 61). It was reported that HO-1 expression and activity are essential for the differentiation of MSCs toward an osteoblastic lineage, as well as vital for their growth (61). In addition, the inhibition of HO-1 favors the differentiation of MSCs toward the formation of adipocytes, with a decrease in osteoblast formation (4, 60, 61).

Although HO-1 induction was demonstrated to impair osteoclast differentiation (17, 34, 71) in transgenic mice, we showed that *Hmox1* deficiency downregulated osteoclast number and activity. These results may appear contradictory at first. However, and taking into account the physiological context, the osteoblastic lineage is the main modulator of osteoclast differentiation and activation, so that the observed

decrease in osteoblast number and activity in *Hmox1*-deficient mice may explain the decrease observed in both bone metabolism and osteoclast differentiation and activation. These results are further supported by the altered expression found in genes involved in osteoblast differentiation and/or regulation of bone physiology, concurrent with the general decrease in bone metabolism.

It was reported that the reduction in ROS levels mediated by HO-1 canonical activity, allowed the restoration of osteoblastic markers (4, 61). The PMOs isolated from the calvaria of mice used in this study showed heterogeneous levels of ROS within each genotype, identifying two populations with Low- and High-ROS levels. In the case of *Hmox1*$^{-/-}$ PMOs, a striking decrease in the ''High'' population was observed, indicating that HO-1 loss might establish a maximum limit in ROS level tolerance for these cells, acting as a positive selection factor on cells with low levels of ROS and therefore with a decreased oxidative metabolism.

Of note, when working with PMOs, it is worth mentioning that the isolation of this particular cell linage requires HO-1 for differentiation (4, 60, 61); hence, *Hmox1* deficiency might also severely impact on the number of PMOs. This evidence is in line with the histomorphometry analysis performed in this work, depicting a decrease in bone metabolism when analyzing the osteoblasts from femurs of KO Hmox1 transgenic mice compared with WT and/or heterozygous femurs. Whether the High-ROS level cell population, during the animal development, did initially exist in abundance and was then lost—unable to survive in a high ROS condition— is still to be elucidated.

Regarding the metastatic process, resorption may be a necessary step for tumor cell homing to bone (69). The consequent bone destruction releases growth factors such as transforming growth factors β (TGF-βs) and BMPs from the mineralized bone matrix, further enhancing tumor growth and survival in a vicious cycle (22). Tumor cells can stimulate osteoclast activity by directly altering the RANKL/OPG ratio, or secreting signaling molecules such as PTHrP to stimulate RANKL production by osteoblast (35, 66).

Considering the involvement of HO-1 in osteoblast differentiation (60), we next studied the effect of cocultures of human PCa cells (pretreated or not with hemin) and the WT or *Hmox1*-deficient PMOs. PCa cell coculture altered PMO gene expression, leading toward a pro-osteoclastogenic profile over an osteoblastic function. Hemin pretreated tumor cells could be modulating the interaction by soluble factors of cancer cells with PMOs, leading toward a more pro-osteoblastic profile. The observed changes on PMOs may be partly explained by the expression changes in *PTHrP* in the tumor cells. PTHrP was first isolated from human carcinomas (26, 29) and it is one of the main agents for the humoral hypercalcemia associated with various malignancies (19).

PTHrP is structurally associated with PTH, a hormone of vital importance in calcium metabolism (53). PTHrP is a key factor in osteolytic bone metastasis, it increases the production of RANKL and decreases the secretion of OPG from the osteoblasts and stromal cells (30), favoring osteoclastogenesis; however, its direct effects on osteoclasts remain elusive. In addition, breast and PCa cells that produce osteolytic metastases (*i.e.*, MDA-MB-231, MDA-MB-435s, PC3) secreted PTHrP (23, 68). These results suggest that PTHrP could play a pivotal role in bone metastases formation and/or development. Conversely, engineered overexpression of PTHrP in breast or PCa cells increased metastases to the bone compartments and osteoclast-mediated bone destruction at the tumor/bone interface (24, 65).

Of note, PTHrP overexpression did not affect the formation of metastases to nonbone sites (24), and a PTHrP neutralizing antibody had no effect on visceral metastases caused by SBC-5 cells (43), suggesting an exclusive role of PTHrP on bone metastases (19). These results highlight the involvement of HO-1 in bone and tumor cell communication mediated by soluble factors. It is well known that PTHrP negatively regulates OPG (32). However, our results showcased that when PMOs, WT, were cocultured with PC3 cells pretreated with hemin, no changes were observed in *PTHrP* in PC3 cells, but *Opg* was downregulated in the PMOs. Thus, *Opg* modulation is clearly affected by other factors. In this regard, DKK1 might be involved in *Opg* downregulation in PMOs. DKK1 stimulates growth and osteolytic bone metastasis in PCa (50, 57).

Patients with multiple myeloma have DKK1 increased levels in the bone compartment, and thus, it has been proposed as an osteoblast suppression mechanism (19, 58). Furthermore, PC3 cells express and release DKK1 and silencing of this molecule resulted in an osteolytic to osteoblastic phenotypic shift (10, 50). DKK1 inhibits OPG release from osteoblasts (50). Thus, the decrease in *Opg* in WT and Het PMOs could be partly explained by the increase in *DKK1* expression in PC3 cells when cocultured with PMOs. On the contrary, a drop in *Opg* expression is also seen in KO PMOs, but in this case, it appears not related to the DKK1 produced by the tumor cell, since no changes are seen in *DKK1* expression in PC3 cells when cocultured with KO PMOs. In line with these results, OPG increases in human bone metastases compared with both primary tumor and nodule metastasis (8). PC3 cells express OPG (28), however, they do so at significantly lower levels compared with bone marrow stromal cells (47). This might suggest that beyond OPG bone function, the observed changes in OPG levels in malignant cells could have direct implications on the tumor since OPG can act as a decoy TRAIL receptor decreasing apoptosis mediated by this factor (27).

Figure 7 summarizes our proposed model on the crosstalk between tumor cells and PMOs, where the increase in PTHrP levels in tumor cells by the coculture stimulates Rankl expression in the PMOs (*Hmox1*$^{+/+}$ and *Hmox1*$^{+/-}$). This mechanism would favor the osteoclast differentiation and activation in the bone microenvironment. Hemin pretreatment of PCa cells interferes in the interaction with bone cells, preventing the stimulation of PTHrP in the tumor cell and the consequent change in Rankl levels in *Hmox1*$^{+/+}$ PMOs, favoring a pro-osteoblastic profile. This modulatory effect is lost when compared with the *Hmox1*$^{+/-}$ PMO coculture, where despite hemin pretreatment, the induction of PTHrP in the tumor cell is maintained and therefore Rankl increases in the *Hmox1*$^{+/-}$ PMOs. Finally, this mechanism results less sensitive in *Hmox1*$^{-/-}$ PMOs, since a greater increase in PTHrP levels in the tumor cell is required for an increase in Rankl levels in the *Hmox1*$^{-/-}$ PMOs to be evident (Fig. 7).

The molecular mechanisms that govern the distortion of the bone remodeling process occurring in metastatic cancer invading the bone are still poorly understood. The present

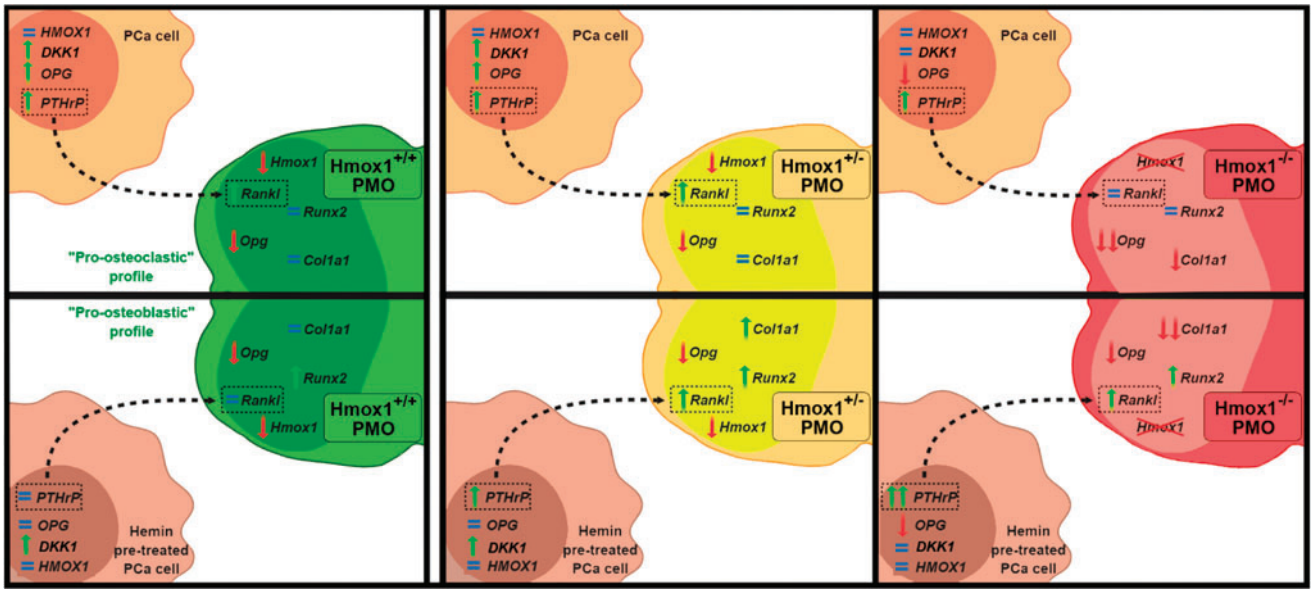

FIG. 7. Schematic representation of the proposed model for the bone-associated genes affected by the crosstalk between tumor cells and PMOs, where the increase in the PTHrP levels in tumor cells due to the coculture could be acting on the PMOs (*Hmox1*$^{+/+}$ and $^{+/-}$), stimulating Rankl expression. This mechanism would favor the osteoclast differentiation and activation in the bone microenvironment. Hemin pretreatment of PCa cells interferes with the interaction with bone cells, preventing the stimulation of PTHrP in the tumor cell and the change in Rankl levels in *Hmox1*$^{+/+}$ PMOs, leading toward a higher pro-osteoblastic profile. This modulatory effect is lost when compared with the coculture with the *Hmox1*$^{+/-}$ PMOs, where despite hemin pretreatment, the induction of PTHrP in the tumor cell is maintained, and therefore, Rankl increases in the *Hmox1*$^{+/-}$ PMOs. This mechanism appears as less sensitive in *Hmox1*$^{-/-}$ PMOs, since a greater increase in PTHrP levels in the tumor cell is needed for an increase in Rankl levels in the *Hmox1*$^{-/-}$ PMOs. PTHrP, parathyroid hormone-related protein. Color images are available online.

results reveal the importance of HO-1 expression in bone, not only for the physiology of bone cells but also in the modulation of the communication between PMOs and PCa cells by soluble factors, where PTHrP/RANKL appear as a critical axis.

Materials and Methods

Animals

All animal experiments were conducted in accordance with the Animal Research: Reporting of *In Vivo* Experiments guidelines. Eight-week-old male BALBc/*Hmox1*$^{+/+}$, *Hmox1*$^{+/-}$ *or Hmox1*$^{-/-}$ mice, initially provided by Dr. Saw Feng-Yet, were housed in the animal facility of the Experimental Obstetrics and Gynecology of the Medical Faculty, Otto-von-Guericke University, Magdeburg.

PMO isolation

PMOs were isolated from the calvaria of mice (three per group per experiment) following the procedure described by Bakker and Klein-Nulend (3), with slight modifications. In brief, after dissection, calvarias were cut into small pieces and digested for 30 min in a shaking incubator at 37°C in 4 mL of α-MEM containing 2 mg/mL collagenase P (Roche Diagnostic GmbH, Mannheim, Germany). After this time, the last step was repeated by renewing the collagenase solution P. Then, the bone pieces were incubated (30 min in a shaking incubator at 37°C) in a solution of 2.5% trypsin plus 0.1% EDTA (Life Technologies, Inc.) in phosphate-buffered saline (PBS). A final incubation with collagenase P solution was performed (30 min in a shaking incubator at 37°C). The bone fragments were rinsed with α-MEM plus penicillin, streptomycin, and 10% fetal bovine serum (FBS). This last procedure was repeated three times, each time. Finally, the bone pieces were plated in three 25 cm^2 flasks containing α-MEM plus penicillin, streptomycin, and 10% FBS. Once the cells migrated from the bone fragments to the plate and reached the desired confluence, they were trypsinized and replated in culture dishes to perform experiments.

Histomorphometric analysis

Mice were euthanized and the dissected bones fixed in buffered 4% formalin (pH: 7.4) for 24 h, rinsed with PBS, and stored in 70% ethanol until processing. Then were embedded in methyl methacrylate plastic resin and cut into consecutive longitudinal sections at 5 micron thickness for histomorphometric analysis. Osteoblast and osteoclast measurements were performed on toluidine blue and acid phosphatase tartrate-resistant (TRAP)/hematoxylin-stained sections, respectively. Measurements were performed on two sections separated by a distance of 40 μm, and then, data were pooled. The region of interest was located at the distal metaphysis of the femur starting 150 μm proximally from the growth plate and extending 1.3 mm toward the diaphysis. The measurement area excluded the 150 μm area adjacent to the cortical bone. On the toluidine blue-stained slides, all cancellous bone endosteal surface lengths were measured and categorized as OS, or osteoblast surface (Ob.S), in the presence or

absence of osteoid. For surfaces identified as osteoblast surface, individual osteoblasts were counted and the data pooled. All other surfaces were considered quiescent. For the TRAP-stained slides, osteoclast surface (Oc.S) and/or erosion surface (ES) were identified, surface lengths measured, and the data pooled. For surface identified as Oc.S., the individual TRAP-positive, multinucleated osteoclasts were counted and the data pooled. Surface that was rough and scalloped in appearance, either with or without the presence of osteoclasts, was categorized as ES. The samples were analyzed using a microscope Leica DM 1000 with a 20× objective, coupled to a Qimaging Bioquant® PV1 Camera for the acquisition of the images (at room temperature; medium: air). The software Bioquant Osteo 2017 was used for imaging and analysis. Images were first captured in Bioquant Image Format (.bif) and then converted to .tif format.

Cell lines

Human PC3 cells (ATCC® CRL-1435) were obtained from the American Type Culture Collection (Manassas, VA) and routinely cultured in RPMI 1640 (Invitrogen, Carlsbad, CA) supplemented with 10% FBS.

Hemin pretreatment of PCa cells and coculture system

An *in vitro* biocompartment culture system was used to study the interaction between PCa cells and bone as previously described and slightly modified (67). Briefly, on day 0, PC3 cells were seeded (100,000 cell/insert) in six-well plate cell culture inserts (0.4-mm pore; Falcon/Becton Dickinson Labware, Franklin Lakes, NJ), and on day 1, they were treated with hemin (50 μM; Sigma-Aldrich, St Louis, MO), a potent specific inducer of HO-1 (Hemin PC3). Controls received fresh medium. The PMOs were also seeded on day 1 in six-well tissue culture plates (200,000 cells/well). On day 2, the inserts containing the PC3 cells (pretreated or not with hemin) were extensively washed with PBS. Then, the inserts were placed into tissue culture plates containing the PMOs so that the two different cell types shared the culture medium but were not in physical contact. Coculturing of PC3 cells with PMOs was performed with α-MEM plus 2% FBS for 24 h. On day 3, the cells were collected and different parameters were analyzed. As control, each cell type (PC3 cells pretreated or not with hemin and PMOs) was grown alone. Cultures were done in triplicate and each experiment was assayed three times.

RNA isolation, complementary DNA synthesis, and quantitative real-time polymerase chain reaction

Total RNA was extracted from cells using the TRIzol® (Life Technologies, Inc.) reagent followed by RNA extraction with chloroform, precipitation with isopropanol, and washing with ethanol. RNA was then diluted in RNA-free water, quantification was performed by ultraviolet absorbance at 260 nm, and quality checked by measuring absorbance at 260/280 nm (Synergy HT; BioTek Instruments). RNA was storaged at −80°C until use. The RNA was reversed transcribed as follows: 2 μg of total RNA was incubated with oligo dTs and RNA-free water 10 min at 75°C and rested 2 min on ice. Incubation for 30 min at 37°C with dNTPs (2.5 mM), DNase I (2 U/μL), and Rnase inhibitor (40 U/μL) in a reaction buffer followed. Afterward, DNAse inactivation for 5 min at 75°C took place. After resting on ice for 2 min, reverse transcriptase (200 U/μL) was added together with Rnase inhibitor (40 U/μL) and complementary DNA (cDNA)-synthesis occurred at 42°C for 60 min. Samples were stored at −20°C subsequent to inactivation of reverse transcriptase for 5 min at 94°C. Real-time polymerase chain reaction (PCR) amplifications were performed with SYBR Green (Applied Biosystems) and an iQ5 Multicolor Real-Time PCR Detection System (BioRad). Each amplification reaction consisted of 1 μL cDNA, 6.5 μL SYBR Green PCR mastermix, 2 μL RNAse free water, 3 μL primer mix, and 0.5 μL fluorescein (50 nM). Primers used are listed in Table 1. PPIA and 36b4 were used as internal reference genes. Data obtained were analyzed using the method of $2^{-\Delta\Delta CT}$ (38).

Assessment of ROS by flow cytometry

After the coculture, the PMOs were washed twice with PBS and incubated with 6 μM 5,6-clorometil-2′7′-dichloro

Table 1. Table of Used Primers Containing the Gene Name, Species, Sequences, and Annealing Temperature

Gene	*Species*	*Primer Fw (5′ > 3′)*	*Primer Rv (5′ > 3′)*	*Annealing temperature (°C)*
36b4	Mouse	AAGCGCGTCCTGGCATTGTCT	CCGCAGGGGCAGCAGTGGT	60
Hmox1	Mouse	AAGAGGCTAAGACCGCCTTC	GCATAAATTCCCACTGCCAC	60
Runx2	Mouse	CCGCACGACAACCGCACCAT	AGGCATTTCGGAGCTCGGCG	60
Rankl	Mouse	ATGGAAGGCTCATGGTTGGATG	AAGAGGACAGAGTGACTTTATGGG	60
Casf1	Mouse	CAACAGCTTTGCTAAGTGCTCTA	CACTGCTAGGGGTGGCTTTA	60
Il-6	Mouse	CTGCAAGAGACTTCCATCCAGTT	GAAGTAGGGAAGGCCGTCG	60
Opg	Mouse	TGCTAATTCAGAAAGGAAATGC	TGGTATAATCTTGGTAGGAACAG	58
Opn	Mouse	TCTCTTGGCTGAATTCTGAGG	CTATAGGATCTGGGTGCAGGC	60
Col1a1	Mouse	CATGTTCAGCTTTGTGGACCT	GCAGCTGACTTCAGGGATGT	60
PPIA	Human	GGTATAAAAGGGGCGGGAGG	CTGCAAACAGCTCAAAGGAGAC	60
HMOX1	Human	ACTGCGTTCCTGCTCAACAT	GGGGCAGAATCTTGCACTTT	60
PTHrP	Human	GTCTCAGCCGCCGCCTCAA	GGAAGAATCGTCGCCGTAAA	60
OPG	Human	GAAGGGCGCTACCTTGAGAT	GCA AACTGTATTTCGCTCTGG	59

Hmox1, heme oxygenase-1 gene.

dihydro-fluorescein diacetate, acetyl ester (CM-H2DCFDA; Invitrogen, Munich, Germany) for 1 h at 37°C. Cells were washed and incubated for 15 min in full medium. Cells were then trypsinized and resuspended with PBS. H2DCFDA levels were measured by flow cytometry in the fluorescein isothiocyanate (FITC) channel (Attune NxT Flow Cytometer; Invitrogen, Munich, Germany) and analyzed with the FlowJo 7.6 software.

Statistical analysis

All results are shown as mean ± standard deviation of three separate independent experiments unless stated otherwise. RT-qPCR data sets were taken as paired samples and analyzed using the repeated measures analysis of variance (ANOVA) model. For other assays, the one-way ANOVA was used. Tukey post-test was used to ascertain statistical significance among the experimental conditions with a threshold of $p < 0.05$ (*), $p < 0.01$ (**), and $p < 0.001$ (***).

For gene expression level correlation analysis, the data were processed for outlier detection using the confidence ellipse method (1).

Acknowledgments

We are grateful to Dr. Mandy Busse for her assistance with the flow cytometry panels and handling, and to Stefanie Langwisch for her assistance with the experiments.

Authors' Contributions

Conception/design: G.G., A.C.Z., and E.V. Provision of reagents and facilities: N.N., A.C.Z., G.G., and E.V. Acquisition of data: N.A., M.S., and E.L. Analysis/interpretation of data: N.A., M.S., N.N., A.C.Z., G.G., and E.V. Writing of the article: N.A., A.C.Z., G.G., and E.V. Review of the article: N.A., N.N., J.C., E.L., G.G., A.C.Z., and E.V. Study supervision: A.C.Z., G.G., and E.V.

Author Disclosure Statement

The authors declare no potential conflicts of interest.

Funding Information

This work was supported by grants from AGENCIA-PICT 2015-1786 (Argentina), AGENCIA-PICT 2016-1366 (Argentina), UBACyT (Argentina), and the National Cancer Institute (Argentina). A.C.Z. received grants from the Deutsche Forschungsgemeinschaft (DFG, ZE 526/12-1). N.A. received a Boehringer Ingelheim Fonds travel grant.

References

1. Alexandersson A. Graphing confidence ellipses: an update of Ellip for Stata 8. *Stata J Promot Commun Stat Stata* 4: 242–256, 2004.
2. Almeida M. Unraveling the role of FoxOs in bone—insights from mouse models. *Bone* 49: 319–327, 2011.
3. Bakker AD and Klein-Nulend J. Osteoblast isolation from murine calvaria and long bones. *Methods Mol Biol* 816: 19–29, 2012.
4. Barbagallo I, Vanella A, Peterson SJ, Kim DH, Tibullo D, Giallongo C, Vanella L, Parrinello N, Palumbo GA, Di Raimondo F, Abraham NG, and Asprinio D. Overexpression of heme oxygenase-1 increases human osteoblast stem cell differentiation. *J Bone Miner Metab* 28: 276–288, 2010.
5. Bonewald LF. The amazing osteocyte. *J Bone Miner Res* 26: 229–238, 2011.
5a. Bray F, Ferlay J, Soerjomataram I, Siegel RL, Torre LA, and Jemal A. Global cancer statistics 2018: GLOBOCAN estimates of incidence and mortality worldwide for 36 cancers in 185 countries. *CA Cancer J Clin* 68: 394–424, 2018.
6. Calvi LM, Sims NA, Hunzelman JL, Knight MC, Giovannetti A, Saxton JM, Kronenberg HM, Baron R, and Schipani E. Activated parathyroid hormone/parathyroid hormone-related protein receptor in osteoblastic cells differentially affects cortical and trabecular bone. *J Clin Invest* 107: 277–286, 2001.
7. Capulli M, Paone R, and Rucci N. Osteoblast and osteocyte: games without frontiers. *Arch Biochem Biophys* 561: 3–12, 2014.
8. Chen G, Sircar K, Aprikian A, Potti A, Goltzman D, and Rabbani SA. Expression of RANKL/RANK/OPG in primary and metastatic human prostate cancer as markers of disease stage and functional regulation. *Cancer* 107: 289–298, 2006.
9. Clarke B. Normal bone anatomy and physiology. *Clin J Am Soc Nephrol* 3(Suppl 3): S131–S139, 2008.
10. Clines KL and Clines GA. DKK1 and Kremen expression predicts the osteoblastic response to bone metastasis. *Transl Oncol* 11: 873–882, 2018.
11. Damoulis PD and Hauschka PV. Nitric oxide acts in conjunction with proinflammatory cytokines to promote cell death in osteoblasts. *J Bone Miner Res* 12: 412–422, 1997.
12. Datta HK, Ng WF, Walker JA, Tuck SP, and Varanasi SS. The cell biology of bone metabolism. *J Clin Pathol* 61: 577–587, 2008.
13. Decker AM, Jung Y, Cackowski F, and Taichman RS. The role of hematopoietic stem cell niche in prostate cancer bone metastasis. *J Bone Oncol* 5: 117–120, 2016.
14. Downey PA and Siegel MI. Bone biology and the clinical implications for osteoporosis. *Phys Ther* 86: 77–91, 2006.
15. Feller L, Kramer B, and Lemmer J. A short account of metastatic bone disease. *Cancer Cell Int* 11: 24, 2011.
16. Ferrando M, Wan X, Meiss R, Yang J, De Siervi A, Navone N, and Vazquez E. Heme oxygenase-1 (HO-1) expression in prostate cancer cells modulates the oxidative response in bone cells. *PLoS One* 8: 1–14, 2013.
17. Florczyk-Soluch U, Józefczuk E, Stępniewski J, Bukowska-Strakova K, Mendel M, Viscardi M, Nowak WN, Józkowicz A, and Dulak J. Various roles of heme oxygenase-1 in response of bone marrow macrophages to RANKL and in the early stage of osteoclastogenesis. *Sci Rep* 8: 1–15, 2018.
18. Florencio-Silva R, Rodrigues da Silva Sasso G, Sasso-Cerri E, Simões MJ, and Cerri PS. Biology of bone tissue: structure, function, and factors that influence bone cells. *Biomed Res Int* 2015: 421746, 2015.
19. Fournier PGJ, Dunn LK, Clines GA, and Guise TA. Tumor-bone cell interactions in bone metastases. In: Heymann D

(ed). *Bone Cancer*, 1st ed. Amsterdam, Netherlands: Elsevier, Inc., 2010, pp. 9–40.
20. Grochot-Przeczek A, Dulak J, and Jozkowicz A. Haem oxygenase-1: non-canonical roles in physiology and pathology. *Clin Sci (Lond)* 122: 93–103, 2012.
21. Gueron G, Giudice J, Valacco P, Paez A, Elguero B, Toscani M, Jaworski F, Leskow FC, Cotignola J, Marti M, Binaghi M, Navone N, and Vazquez E. Heme-oxygenase-1 implications in cell morphology and the adhesive behavior of prostate cancer cells. *Oncotarget* 5: 4087–4102, 2014.
22. Guise TA, Mohammad KS, Clines G, Stebbins EG, Wong DH, Higgins LS, Vessella R, Corey E, Padalecki S, Suva L, and Chirgwin JM. Basic mechanisms responsible for osteolytic and osteoblastic bone metastases. *Clin Cancer Res* 12: 6213–6217, 2006.
23. Guise TA, Yin JJ, Taylor SD, Kumagai Y, Dallas M, Boyce BF, Yoneda T, and Mundy GR. Evidence for a causal role of parathyroid hormone-related protein in the pathogenesis of human breast cancer-mediated osteolysis. *J Clin Invest* 98: 1544–1549, 1996.
24. Guise TA, Yin JJ, Thomas RJ, Dallas M, Cui Y, and Gillespie MT. Parathyroid hormone-related protein (PTHrP)-(1–139) isoform is efficiently secreted in vitro and enhances breast cancer metastasis to bone in vivo. *Bone* 30: 670–676, 2002.
25. Han Y, You X, Xing W, Zhang Z, and Zou W. Paracrine and endocrine actions of bone—the functions of secretory proteins from osteoblasts, osteocytes, and osteoclasts. *Bone Res* 1: 1–11, 2018.
26. Hanai J, Chen LF, Kanno T, Ohtani-Fujita N, Kim WY, Guo WH, Imamura T, Ishidou Y, Fukuchi M, Shi MJ, Stavnezer J, Kawabata M, Miyazono K, and Ito Y. Interaction and functional cooperation of PEBP2/CBF with Smads. Synergistic induction of the immunoglobulin germline Calpha promoter. *J Biol Chem* 274: 31577–31582, 1999.
27. Holen I, Croucher PI, Hamdy FC, and Eaton CL. Osteoprotegerin (OPG) is a survival factor for human prostate cancer cells. *Cancer Res* 62: 1619–1623, 2002.
28. Holen I and Shipman CM. Role of osteoprotegerin (OPG) in cancer. *Clin Sci* 110: 279–291, 2006.
29. Janknecht R, Wells NJ, and Hunter T. TGF-beta-stimulated cooperation of smad proteins with the coactivators CBP/p300. *Genes Dev* 12: 2114–2119, 1998.
30. Janssens K, ten Dijke P, Janssens S, and Van Hul W. Transforming growth factor-beta1 to the bone. *Endocr Rev* 26: 743–774, 2005.
31. This reference has been deleted.
32. Jin JK, Dayyani F, and Gallick GE. Steps in prostate cancer progression that lead to bone metastasis. *Int J Cancer* 128: 2545–2561, 2011.
33. Karsenty G, Kronenberg HM, and Settembre C. Genetic control of bone formation. *Annu Rev Cell Dev Biol* 25: 629–648, 2009.
34. Ke K, Safder MA, Sul OJ, Kim WK, Suh JH, Joe Y, Chung HT, and Choi HS. Hemeoxygenase-1 maintains bone mass via attenuating a redox imbalance in osteoclast. *Mol Cell Endocrinol* 409: 11–20, 2015.
35. Keller ET and Brown J. Prostate cancer bone metastases promote both osteolytic and osteoblastic activity. *J Cell Biochem* 91: 718–729, 2004.
36. Khosla S, Oursler MJ, and Monroe DG. Estrogen and the skeleton. *Trends Endocrinol Metab* 23: 576–581, 2012.
37. Li ZG, Yang J, Vazquez ES, Rose D, Vakar-Lopez F, Mathew P, Lopez A, Logothetis CJ, Lin S-H, and Navone NM. Low-density lipoprotein receptor-related protein 5 (LRP5) mediates the pro state cancer-induced formation of new bone. *Oncogene* 27: 596–603, 2008.
38. Livak KJ and Schmittgen TD. Analysis of relative gene expression data using real-time quantitative PCR and the 2(-delta delta C(T)) method. *Methods* 25: 402–408, 2001.
39. Loboda A, Damulewicz M, Pyza E, Jozkowicz A, and Dulak J. Role of Nrf2/HO-1 system in development, oxidative stress response and diseases: an evolutionarily conserved mechanism. *Cell Mol Life Sci* 73: 3221–3247, 2016.
40. Logothetis CJ, Gallick GE, Maity SN, Kim J, Aparicio A, Efstathiou E, and Lin SH. Molecular classifi cation of prostate cancer progression: foundation for marker-driven treatment of prostate cancer. *Cancer Discov* 3: 849–861, 2013.
41. De Marzo AM, Platz EA, Sutcliffe S, Xu J, Gronberg H, Drake CG, Nakai Y, Isaacs WB, and Nelson WG. Inflammation in prostate carcinogenesis. *Nat Rev Cancer* 7: 256–269, 2007.
42. Matsuo K and Irie N. Osteoclast-osteoblast communication. *Arch Biochem Biophys* 473: 201–209, 2008.
43. Miki T, Yano S, Hanibuchi M, Kanematsu T, Muguruma H, and Sone S. Parathyroid hormone-related protein (PTHrP) is responsible for production of bone metastasis, but not visceral metastasis, by human small cell lung cancer SBC-5 cells in natural killer cell-depleted SCID mice. *Int J Cancer* 108: 511–515, 2004.
44. Mundy GR. Metastasis to bone: causes, consequences and therapeutic opportunities. *Nat Rev Cancer* 2: 584–593, 2002.
45. Niida A, Hiroko T, Kasai M, Furukawa Y, Nakamura Y, Suzuki Y, Sugano S, and Akiyama T. DKK1, a negative regulator of Wnt signaling, is a target of the β-catenin/TCF pathway. *Oncogene* 23: 8520–8526, 2004.
46. Nitti M, Piras S, Marinari U, Moretta L, Pronzato M, and Furfaro A. HO-1 induction in cancer progression: a matter of cell adaptation. *Antioxidants* 6: 29, 2017.
47. Nyambo R, Cross N, Lippitt J, Holen I, Bryden G, Hamdy FC, and Eaton CL. Human bone marrow stromal cells protect prostate cancer cells from TRAIL-induced apoptosis. *J Bone Miner Res* 19: 1712–1721, 2004.
48. Paez A, Vazquez E, and Gueron G. Heme oxygenase 1 governs the cytoskeleton at filopodia: pulling the brakes on the migratory capacity of prostate tumoral cells. *Cell Death Discov* 3: 17020, 2017.
49. Park JH, Lee NK, and Lee SY. Current understanding of RANK signaling in osteoclast differentiation and maturation. *Mol Cells* 40: 706–713, 2017.
50. Pinzone JJ, Hall BM, Thudi NK, Vonau M, Qiang YW, Rosol TJ, and Shaughnessy JD. The role of Dickkopf-1 in bone development, homeostasis, and disease. *Blood* 113: 517–525, 2009.
51. Pittenger MF, Mackay AM, Beck SC, Jaiswal RK, Douglas R, Mosca JD, Moorman MA, Simonetti DW, Craig S, and Marshak DR. Multilineage potential of adult human mesenchymal stem cells. *Science* 284: 143–147, 1999.

52. Robling AG, Castillo AB, and Turner CH. Biomechanical and molecular regulation of bone remodeling. *Annu Rev Biomed Eng* 8: 455–498, 2006.
53. Schilling AF, Priemel M, Timo Beil F, Haberland M, Holzmann T, Catalá-Lehnen P, Pogoda P, Blicharski D, Müldner C, Löcherbach C, Rueger JM, and Amling M. Transgenic and knock out mice in skeletal research. Towards a molecular understanding of the mammalian skeleton. *J Musculoskelet Neuronal Interact* 1: 275–27589, 2001.
54. Suva LJ, Washam C, Nicholas RW, and Griffin RJ. Bone metastasis: mechanisms and therapeutic opportunities. *Nat Rev Endocrinol* 7: 208–218, 2011.
55. Szade K, Zukowska M, Szade A, Nowak W, Skulimowska I, Ciesla M, Bukowska-Strakova K, Gulati GS, Kachamakova-Trojanowska N, Kusienicka A, Einwallner E, Kijowski J, Czauderna S, Esterbauer H, Benes V, Weissman I, Dulak J, and Jozkowicz A. Heme oxygenase-1 deficiency triggers exhaustion of hematopoietic stem cells. *EMBO Rep* 2019. [Epub ahead of print]; DOI: 10.15252/embr.201947895.
56. Teitelbaum SL. Osteoclasts: what do they do and how do they do it? *Am J Pathol* 170: 427–435, 2007.
57. Thudi NK, Martin CK, Murahari S, Shu SS, Lanigan LG, Werbeck JL, Keller ET, Mccauley LK, Pinzone JJ, and Rosol TJ. Growth and metastasis and inhibited bone. 71: 615–625, 2011.
58. Tian E, Zhan F, Walker R, Rasmussen E, Ma Y, Barlogie B, and Shaughnessy JDJ. The role of the Wnt-signaling antagonist DKK1 in the development of osteolytic lesions in multiple myeloma. *N Engl J Med* 349: 2483–2494, 2003.
59. Vanderschueren D, Vandenput L, Boonen S, Lindberg MK, Bouillon R, and Ohlsson C. Androgens and bone. *Endocr Rev* 25: 389–425, 2004.
60. Vanella L, Kim DH, Asprinio D, Peterson SJ, Barbagallo I, Vanella A, Goldstein D, Ikehara S, and Abraham NG. HO-1 expression increases mesenchymal stem cell-derived osteoblast. *Bone* 46: 236, 2010.
61. Vanella L, Sanford C, Kim DH, Abraham NG, and Ebraheim N. Oxidative stress and heme oxygenase-1 regulated human mesenchymal stem cells differentiation. *Int J Hypertens* 2012: 890671, 2012.
62. Wan X, Corn PG, Yang J, Palanisamy N, Starbuck MW, Efstathiou E, Li Ning Tapia EM, Zurita AJ, Aparicio A, Ravoori MK, Vazquez ES, Robinson DR, Wu Y-M, Cao X, Iyer MK, McKeehan W, Kundra V, Wang F, Troncoso P, Chinnaiyan AM, Logothetis CJ, and Navone NM. Prostate cancer cell-stromal cell crosstalk via FGFR1 mediates antitumor activity of dovitinib in bone metastases. *Sci Transl Med* 6: 252ra122, 2014.
63. Wauquier F, Leotoing L, Coxam V, Guicheux J, and Wittrant Y. Oxidative stress in bone remodelling and disease. *Trends Mol Med* 15: 468–477, 2009.
64. Wei J, Shimazu J, Makinistoglu MP, Maurizi A, and Karsenty G. Glucose uptake and Runx2 synergize to orchestrate osteoblast differentiation and bone formation. *Cell* 161: 1576–1591, 2015.
65. Wong SK, Mohamad NV, Giaze TR, Chin KY, Mohamed N, and Ima-Nirwana S. Prostate cancer and bone metastases: the underlying mechanisms. *Int J Mol Sci* 20, 2019.
66. Wu JB, Yin L, Shi C, Li Q, Duan P, Huang J-M, Liu C, Wang F, Lewis M, Wang Y, Lin T-P, Pan C-C, Posadas EM, Zhau HE, and Chung LWK. MAOA-dependent activation of Shh-IL6-RANKL Signaling network promotes prostate cancer metastasis by engaging tumor-stromal cell interactions. *Cancer Cell* 31: 368–382, 2017.
67. Yang J, Fizazi K, Peleg S, Sikes CR, Raymond AK, Jamal N, Hu M, Olive M, Martinez LA, Wood CG, Logothetis CJ, Karsenty G, and Navone NM. Prostate cancer cells induce osteoblast differentiation through a Cbfa1-dependent pathway. *Cancer Res* 61: 5652–5659, 2001.
68. Yin JJ, Mohammad KS, Kakonen SM, Harris S, Wu-Wong JR, Wessale JL, Padley RJ, Garrett IR, Chirgwin JM, and Guise TA. A causal role for endothelin-1 in the pathogenesis of osteoblastic bone metastases. *Proc Natl Acad Sci U S A* 100: 10954–10959, 2003.
69. Yonou H-2004-T pdfoyuk., Ochiai A, Goya M, Kanomata N, Hokama S, Morozumi M, Sugaya K, Hatano T, and Ogawa Y. Intraosseous growth of human prostate cancer in implanted adult human bone: relationship of prostate cancer cells to osteoclasts in osteoblastic metastatic lesions. *Prostate* 58: 406–413, 2004.
70. Zaidi M, Inzerillo AM, Moonga BS, Bevis PJR, and Huang CL-H. Forty years of calcitonin—where are we now? A tribute to the work of Iain Macintyre, FRS. *Bone* 30: 655–663, 2002.
71. Zwerina J, Tzima S, Hayer S, Redlich K, Hoffmann O, Henslik-Schnabel B, Smolen JS, Kollias G, and Schett G. Heme oxygenase 1 (HO-1) regulates osteoclastogenesis and bone resorption. *FASEB J* 19: 2011–2013, 2005.

Address correspondence to:
Dr. Geraldine Gueron
Departamento de Química Biológica
Facultad de Ciencias Exactas y Naturales
Universidad de Buenos Aires (UBA)
Instituto de Química Biológica de la Facultad de Ciencias Exactas y Naturales (IQUIBICEN)
UBA—CONICET
Intendente Guiraldes 2160
CP1428 Buenos Aires
Argentina

E-mail: ggueron@gmail.com

Prof. Ana C. Zenclussen
Experimental Obstetrics and Gynecology
Medical Faculty
Otto-von-Guericke University Magdeburg
Gerhart-Hauptmann-Str 35 39108
Magdeburg
Germany

E-mail: ana.zenclussen@med.ovgu.de

Prof. Elba Vazquez
Departamento de Química Biológica
Facultad de Ciencias Exactas y Naturales
Universidad de Buenos Aires (UBA)
Instituto de Química Biológica de la Facultad de Ciencias Exactas y Naturales (IQUIBICEN)
UBA—CONICET
Intendente Guiraldes 2160
CP1428 Buenos Aires
Argentina

E-mail: elba@qb.fcen.uba.ar

Date of first submission to ARS Central, September 13, 2019; date of final revised submission, December 10, 2019; date of acceptance, December 18, 2019.

Abbreviations Used

ANOVA = analysis of variance
BMPs = bone morphogenetic proteins
cDNA = complementary DNA
DKK1 = inhibitor of Wnt/β-catenin pathway in bone remodeling
ES = erosion surface
FBS = fetal bovine serum
H2DCFDA = 2′7′-dichloro dihydro-fluorescein diacetate
Het = heterozygous
Hmox1 = heme oxygenase-1 gene
HO-1 = heme oxygenase-1
IL = interleukin
KO = knockout
MSCs = mesenchymal stem cells
Oc.S/BS = osteoclast surface/bone surface
OPG = osteoprotegerin
OS = osteoid surface
PBS = phosphate-buffered saline
PCa = prostate cancer
PCR = polymerase chain reaction
PMOs = primary mouse osteoblasts
PTH = parathyroid hormone
PTHrP = parathyroid hormone-related protein
RANKL = receptor activator for nuclear factor κ B ligand
ROS = reactive oxygen species
TRAP = acid phosphatase tartrate resistant
WT = wild type